

# REPORT DOCUMENTATION PAGE

The public reporting burden for this collection of information is estimated to average 1 hour per response, including gathering and maintaining the data needed, and completing and reviewing the collection of information. Send comments regarding this burden estimate or any other aspect of this collection of information, including suggestions for reducing the burden, to the Department of Defense, Executive Service Administration, Paperwork Project, Washington, DC 20301-4070. Send all other correspondence regarding this collection of information to the Office of Management and Budget, Paperwork Project, Washington, DC 20503-2940.

AFRL-SR-AR-TR-05-

0058

ces,  
on of  
ware  
OMB

PLEASE DO NOT RETURN YOUR FORM TO THE ABOVE ORGANIZATION.

1. REPORT DATE (DD-MM-YYYY) 29-11-2004			2. REPORT TYPE FINAL		3. DATES COVERED (From - To) June 2003 - May 2004	
4. TITLE AND SUBTITLE Advances in Biomagnetic Interfacing Concepts Derived from Polymer-Magnetic Particle Complexes					5a. CONTRACT NUMBER F49620-03-1-0332	
					5b. GRANT NUMBER	
					5c. PROGRAM ELEMENT NUMBER	
6. AUTHOR(S) Zalich, Michael      Gorham, Nicole Connolly, Joan      St. Pierre, Tim, G Harris, Linda Gilbert, Elliot Saunders, Martin					5d. PROJECT NUMBER	
					5e. TASK NUMBER	
					5f. WORK UNIT NUMBER	
7. PERFORMING ORGANIZATION NAME(S) AND ADDRESS(ES) The University Of Western Australia 35 Stirling Hwy Crawley WA 6009 Australia					8. PERFORMING ORGANIZATION REPORT NUMBER	
9. SPONSORING/MONITORING AGENCY NAME(S) AND ADDRESS(ES) USAF, AFRL Office of Scientific Research 4015 Wilson Blvd Room 713 Arlington VA 22203-1954					10. SPONSOR/MONITOR'S ACRONYM(S) AFOSR USAF AFRL	
					11. SPONSOR/MONITOR'S REPORT NUMBER(S)	
12. DISTRIBUTION/AVAILABILITY STATEMENT Approved for public release; distribution is unlimited						
13. SUPPLEMENTARY NOTES						
14. ABSTRACT This report describes the physical characterization of cobalt nanoparticles formed using (1) polysiloxane copolymer micelles and (2) poly(styrene-b-4-vinylphenoxyphthalonitrile) copolymer solutions. Formation of silica coatings around the cobalt nanoparticles is shown to protect the cobalt from oxidation in aerobic environments. Native particles have a narrow particle size distribution while pyrolyzed particles appear to comprise a bimodal or broader distribution of sizes. Pyrolysis of the native sample increases the cobalt specific saturation magnetization. Native cobalt nanoparticles formed in poly(styrene-b-4-vinylphenoxyphthalonitrile) copolymer solutions are weakly crystalline while their pyrolyzed counterparts have a high degree of crystallinity. Pyrolysis increases the cobalt specific saturation magnetization from approximately 80 emu/g Co to values close to that observed for bulk cobalt (160 emu/g Co). The formation of a graphitic coating around the cobalt nanoparticles upon pyrolysis appears to prevent oxidation of the cobalt in air.						
15. SUBJECT TERMS Cobalt nanoparticles, magnetic susceptibility, polymer						
16. SECURITY CLASSIFICATION OF:			17. LIMITATION OF ABSTRACT	18. NUMBER OF PAGES	19a. NAME OF RESPONSIBLE PERSON	
a. REPORT UU	b. ABSTRACT UU	c. THIS PAGE UU			Timothy G. St. Pierre	
					19b. TELEPHONE NUMBER (Include area code) +61 8 6488 2747	

# **Advances in Bio-Magnetic Interfacing Concepts derived from Polymer-Magnetic Particle Complexes**

A project funded by AFOSR-DARPA  
1<sup>st</sup> June 2003 to 31<sup>st</sup> May 2004

Final report from School of Physics at The University of Western Australia  
November 2004

**Principle Investigator: A/Prof Tim St Pierre**

**Institution: The University of Western Australia, 35 Stirling Hwy, WA 6009, Australia**

**Agreement number: F49620-03-1-0332**

The work presented in this report was carried out by the following Australian based personnel in collaboration with Prof Judy Riffle's research team at Virginia Tech:

Michael Zalich  
Dr Joan Connolly  
Dr Linda Harris  
Dr Elliot Gilbert  
Dr Martin Saunders  
Nicole Gorham  
A/Prof Tim St Pierre

20050308 076

## Table of Contents

<b>ADVANCES IN BIO-MAGNETIC INTERFACING CONCEPTS DERIVED FROM POLYMER-MAGNETIC PARTICLE COMPLEXES .....</b>	<b>1</b>
TABLE OF CONTENTS .....	2
OBJECTIVES .....	3
<i>Work Statement</i> .....	3
<i>Status of Effort</i> .....	3
ACCOMPLISHMENTS / NEW FINDINGS .....	4
<i>Overview</i> .....	4
<i>Cobalt nanoparticles formed in polysiloxane copolymer micelles: effect of production methods on magnetic properties</i> .....	4
<i>Block copolysiloxanes and their complexation with cobalt nanoparticles</i> .....	8
<i>Cobalt nanoparticles formed in poly(styrene-b-4-vinylphenoxyphthalonitrile) copolymer solutions: effect of pyrolysis on magnetic properties</i> .....	11
REFERENCES .....	18
PERSONNEL .....	19
PUBLICATIONS.....	19
INTERACTIONS/TRANSITIONS .....	19
NEW DISCOVERIES, INVENTIONS, PATENT DISCLOSURES.....	20

## Objectives

### Work Statement

**Task 1:** Magnetic measurements will be made on controlled size magnetite particles in the 10-500 nm diameter size range synthesized at Virginia Tech through (a) base hydrolysis of iron salts and (b) controlled nucleation and crystal growth in the presence of alcohols and carboxylic acids. Measurements will include (1) temperature dependent zero-field-cooled and field-cooled magnetization (2) zero-field-cooled and field-cooled field dependent magnetization (3) magnetic energy barrier distributions. The data from (2) and (3) will be modeled to obtain information of the fraction of atoms in surface states and the chemical speciation of magnetic atoms within each sample. Information on the magnetic properties of surface atoms will be related to the chemical nature of the coatings used in each preparation. Data from (1) and (3) will be used to gain information on interparticle interactions.

**Task 2:** Magnetic measurements equivalent to those in Task 1 will be made on cobalt nanoparticles synthesized at Virginia Tech. Measurements will also be repeated at time intervals of several weeks and under varying ambient oxidative conditions in order to establish the oxidative stability of the magnetic properties. Both field-cooled field dependent magnetization and zero-field-cooled magnetization measurements will be used to establish the degree of oxidation of the cobalt nanoparticles.

**Task 3:** Small angle x-ray scattering measurements will be made on suspensions of both magnetite and cobalt nanoparticle suspensions before and after application of magnetic fields in order to characterize the degree of aggregation of particles.

### Status of Effort

**Task 1:** Preliminary measurements were made on controlled size magnetite particles. Results were published in Chemistry of Materials (Harris et al. 2003). Subsequent development of the technique of pyrolysis of cobalt nanoparticles for improved magnetic properties resulted in a greater emphasis on the cobalt-polymer systems.

**Task 2:** Magnetic measurements have been completed on a series of cobalt-polymer nanoparticulate systems synthesized using polysiloxane copolymer micelles or poly(styrene-*b*-4-vinylphenoxyphthalonitrile) copolymer solutions in both the native and pyrolyzed states. Each system has also been characterized by transmission electron microscopy, electron diffraction, and electron energy loss spectroscopy.

**Task 3:** Small angle x-ray scattering measurements have been made on both native and pyrolyzed cobalt nanoparticles. In addition small angle neutron scattering studies have been carried out on a cobalt nanoparticle-polysiloxane fluid system in zero and applied fields in order to study the aggregation properties of the particles in moderate applied magnetic fields.

## Accomplishments / New Findings

### Overview

This report focuses on the physical characterization of cobalt nanoparticles formed using

- 1) Polysiloxane copolymer micelles
- 2) Poly(styrene-*b*-4-vinylphenoxyphthalonitrile) copolymer solutions

The report summarizes work that has been carried out in collaboration with Prof Judy Riffle at Virginia Tech and that has been published/submitted for publication in the following research papers:

- Vadala, M.L., Zalich, M.A., Fulks, D.B., St. Pierre, T.G., Dailey, J.P., and Riffle, J.S. (2004) Cobalt-silica magnetic nanoparticles with functional surfaces. *J. Mag. Magn. Mat.*, submitted.
- Baranauskas III, V.V., Zalich, M.A., Saunders, M., St. Pierre, T.G., and Riffle, J.S. (2004) Poly(styrene-*b*-4-vinylphenoxyphthalonitrile)-cobalt complexes and their conversion to oxidatively-stable cobalt nanoparticles. *Chem. Mater.*, submitted.
- Vadala, M.L., Rutnakornpituk, M., Zalich, M.A., St. Pierre, T.G., and Riffle, J.S. (2004) Block copolysiloxanes and their complexation with cobalt nanoparticles. *Polymer*, 45, 7449-7461.
- Connolly, J., St. Pierre, T.G., Rutnakornpituk, M., Riffle, J.S. (2004) Cobalt nanoparticles formed in polysiloxane copolymer micelles: effect of production methods on magnetic properties. *J. Phys. D: Appl. Phys.*, 37, 2475-2482.

All materials in this report were synthesized in the laboratories at Virginia Tech under the supervision of Prof Judy Riffle.

### Cobalt nanoparticles formed in polysiloxane copolymer micelles: effect of production methods on magnetic properties.

The effect of production method on the chemical and magnetic stability of a range of cobalt nanoparticles formed in polysiloxane copolymer micelles has been studied. Details of the production methods can be found in progress reports from Prof Judy Riffle and elsewhere (Connolly et al. 2004). The nanoparticles were suspended in polydimethylsiloxane (PDMS) carrier fluids.

The six fluids studied consisted of suspensions of cobalt nanoparticles in PDMS fluids. Two of the fluids (A and B) were stabilized against aggregation by a triblock copolymer: poly [dimethylsiloxane-*b*-(3-cyanopropyl) methylsiloxane-*b*-dimethylsiloxane] (15 000 g mol<sup>-1</sup> PDMS–2000 g mol<sup>-1</sup> PCPMS–15 000 g mol<sup>-1</sup> PDMS). The central polymer block was coordinated to the cobalt particles through CN–Co interactions, and the two outer blocks acted as tails to increase dispersion stability. The dispersion of cobalt nanoparticles in the remaining four fluids utilized a pentablock copolymer stabilizer with an identical central coordinating anchor block (PCPMS), which was flanked by two blocks that served as silica-like precursors, and then by PDMS tailblocks (15 000 g mol<sup>-1</sup> PDMS–5800 g mol<sup>-1</sup> poly(methyltriethoxysilylethylsiloxane) (PMTEOS)–2000 g mol<sup>-1</sup> PCPMS–5800 g mol<sup>-1</sup> PMTEOS–15 000 g mol<sup>-1</sup> PDMS). The PMTEOS block was designed to crosslink around the cobalt surfaces after the production of the fluids and thereby form a 'silica-like' coating around the cobalt nanoparticles to protect them against oxidation. The cobalt particles were prepared by thermally decomposing Co<sub>2</sub>(CO)<sub>8</sub> in toluene or PDMS containing the block copolymers. Samples A and B were prepared in toluene in the

presence of the PDMS-PCPMS-PDMS triblock copolymer and then transferred to PDMS fluid after the synthesis. Samples C and D were prepared in PDMS in the presence of the PDMS-PMTEOS-PCPMS-PMTEOS-PDMS copolymer. Samples E and F were prepared in toluene in the presence of the PDMS-PMTEOS-PCPMS-PMTEOS-PDMS copolymer and then transferred to PDMS. Thus, three families of fluids were studied, and in each case one fluid was sealed in glass under air, and another was sealed in glass under an argon atmosphere. Descriptions of the fluids are summarized in Table 1.

Table 1.

Fluid Label	Production Method	Exposure	% cobalt
A	toluene, no coating	air	1.9
B	toluene, no coating	argon	1.6
C	PDMS, silica coating	air	1.6
D	PDMS, silica coating	argon	1.6
E	toluene, silica coating	air	2
F	toluene, silica coating	argon	2

Magnetic measurements indicate that the silica coating effectively protects the cobalt particles from on-going oxidation with little change in the saturation magnetisation of the particles observed over time (Figure 1). Field-cooled magnetization vs applied field loops have been measured and are used to detect the presence of a cobalt oxide layer in contact with the cobalt. Antiferromagnetic cobalt oxide in contact with ferromagnetic cobalt results in low temperature field-cooled hysteresis loops being shifted relative to their zero-field-cooled counterparts as illustrated in Figure 2.

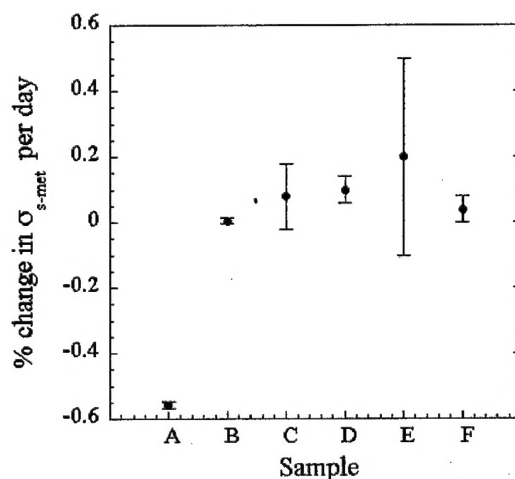


**Figure 1.** Loss per day of specific magnetization of the metallic cobalt component,  $\sigma_{s-met}$ .

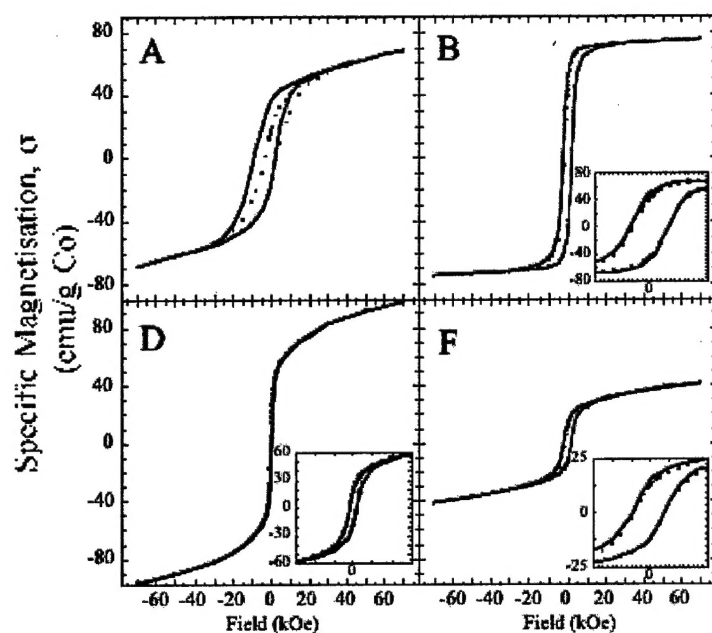


**Figure 2.** Magnetic hysteresis loops for cobalt nanoparticles measured at 5 K after cooling in zero field (closed circles) and in 70 kOe field (line). The letters on the plots refer to the samples measured (Table 1). The inset in each plot is a magnification of fields from -6 kOe to +6 kOe enabling the shifts in the field-cooled loops to be seen more clearly.

Measurements of the loop-shift (or bias field) for all of the samples prepared shows that the silica coating prevents formation of a significant oxide layer even in the presence of air (Figure 3).

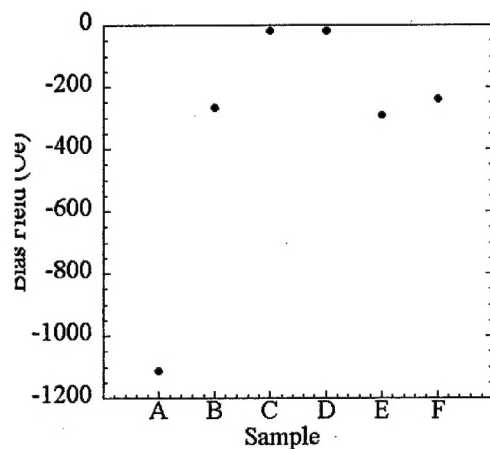


**Figure 3.** The field-cooled magnetic hysteresis loop bias field shift for all samples at 5 K.

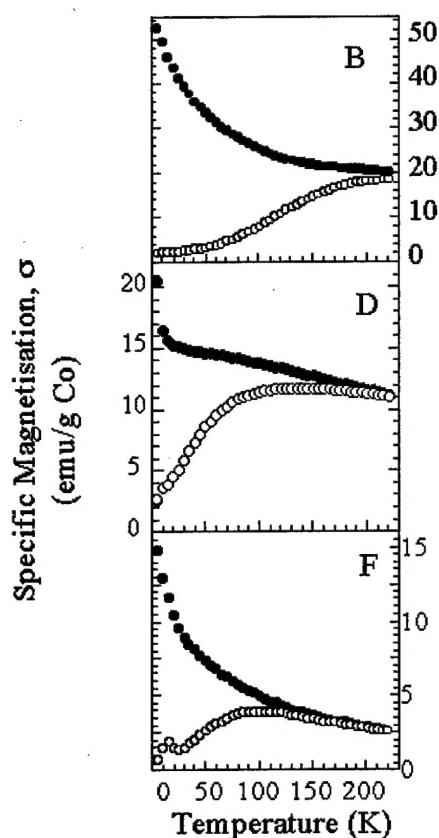


**Figure 4.** Temperature dependent magnetisations in 100 Oe after cooling in zero field (open circles) and in 70 kOe field (closed circles). The letters on the plots refer to the sample measured.

magnetic scattering. We measured the scattering in both the zero-field-cooled (ZFC) and field-cooled (FC) states at a temperature of 100K and at 300K in a fields of 0 and 1 Tesla.

Figure 5 shows a 2D plot for the intermediate  $q$  setting that has been generated from the subtraction of spin up (flipper off) from spin down (flipper on) scattering. This process highlights the nuclear-magnetic cross-term.

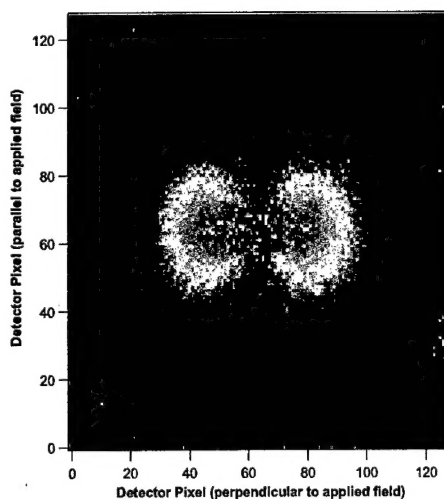


**Figure 5** SANS pattern generated from  $I^-$  (flipper on) -  $I^+$  (flipper off) from field cooled cobalt ferrofluid at 100K in 1 T field showing nuclear-magnetic cross-term.

Temperature dependent magnetisation measurements (Figure 4) show that the silica-coated particles have blocking temperatures of 100-130 K compared to the non-silica coated particles which do not reach their blocking temperature below the melting point of the frozen fluids. This result is interpreted as a smaller magnetic core size in the silica-coated particles. The zero-field-cooled temperature dependent magnetisation of the silica-coated particles has two apparent blocking temperatures with a second, lower blocking temperature of approximately 15 K. This second apparent blocking temperature may be due to unreacted cobalt clusters in the suspensions or alternatively to surface states on the nanoscale cobalt particles.

Small angle neutron scattering (SANS) measurements have been made on a sample of the cobalt nanoparticle suspension in PDMS in order to determine the degree to which clustering of the nanoparticles occurs in an applied field and the degree to which the clustering is reversible once the applied field is removed. In these experiments, performed on the V4 instrument at the Berlin Neutron Scattering Center at the Hahn-Meitner Institute, we have studied a cobalt ferrofluid at a field of 1 T and have also employed polarised neutrons with the aim of more effectively separating the nuclear and



In summary, the silica coating effectively protects the cobalt particles from ongoing oxidation, with little change in the saturation magnetization of the particles observed over time and only a small shift in the centre of the field-cooled hysteresis loop observed. Temperature-dependent magnetization measurements show that the silica-coated particles have superparamagnetic blocking temperatures of 100–130 K compared with the non-silica-coated particles, which do not reach their characteristic blocking temperature below the melting point of the frozen fluids. This result is interpreted as a smaller magnetic core size in the silica-coated particles. The zero-field-cooled temperature-dependent magnetization of the silica-coated particles has two apparent superparamagnetic blocking temperatures, with a second, lower blocking temperature of approximately 15 K. This second apparent blocking temperature may be due to unreacted cobalt clusters in the suspensions or, alternatively, due to surface states on the nanoscale cobalt particles.

### Block copolysiloxanes and their complexation with cobalt nanoparticles

Poly(dimethylsiloxane-*b*-methylvinylsiloxane) (PDMS-*b*-PMVS) diblock copolymers were synthesized in Prof Judy Riffle's laboratory via anionic living polymerization with controlled molecular weights and narrow molecular weight distributions (see Report from Prof Judy Riffle and elsewhere (Vadala et al. 2004)). The PMVS blocks were functionalized with trimethoxysilyl pendent groups to yield poly(dimethylsiloxane-*b*-(methylvinyl-co-methyl(2-trimethoxysilyl)siloxane) (PDMS-*b*-(PMVS-co-PMTMS)) copolymer.

Stable suspensions of mostly superparamagnetic cobalt nanoparticles were prepared in toluene in the presence of PDMS-*b*-(PMVS-co-PMTMS) copolymer via thermolysis of  $\text{Co}_2(\text{CO})_8$ . The suspensions were stored under argon. TEM micrographs showed non-aggregated cobalt nanoparticles with mean particle diameters ranging from ~10–15 nm (Figure 6a). Specific saturation magnetizations of the cobalt-copolymer complexes at room temperature ranged from ~40–110 emu g<sup>-1</sup> of cobalt.

Room temperature and 5 K magnetic susceptibility measurements were used to investigate any presence of: (1) a cobalt oxide layer on the surface of the cobalt nanoparticles and (2) unreacted cobalt carbonyl species in the cobalt-polymer complexes (Figure 7). The cobalt specific magnetization ( $\sigma$ ) shows a continuous increase with field at high fields and low temperature. However, at room temperature  $\sigma$  almost saturates at high fields. These observations are indicative of the presence of paramagnetic species within the sample. This paramagnetic component is believed to be cobalt carbonyl species that have not been incorporated into the cobalt nano-crystals. This observation is in agreement with the infrared spectra, which suggest residual carbon monoxide ligands are present after formation of the cobalt nanoparticle dispersions. It is anticipated that these residual paramagnetic cobalt species will be reacted in subsequent annealing steps for these materials. In addition, the field-cooled 5 K hysteresis loop does not show a large shift from the zero field-cooled hysteresis loop, indicating that there is no significant oxide layer on the surface of the metallic cobalt nanoparticles. If cobalt oxide were present in any significant amount, an asymmetric field-cooled hysteresis loop shift, caused by the coupling of an antiferromagnetic layer (CoO) with a ferromagnetic layer (Co), would be expected (Nogues and Schuller 1999). Subsequent exposure of the cobalt nanoparticles to an aerobic environment induces a significant loop shift in the field-cooled magnetic hysteresis loop indicating the onset of surface oxidation.

Samples of the cobalt-copolymer complexes were pyrolyzed at 600°C under argon for two hours. TEM of thin sections of the resultant material showed a bimodal distribution of particle sizes of cobalt (Figures 6 B,E,F). High resolution TEM of the pyrolyzed material showed lattice planes (Figure 6 C). Fourier transforms of the lattice plane images indicated that some of the cobalt particles had a single crystal nature (Figure 6 C and D). Measurements of cobalt specific magnetization against applied field at room temperature and 5 K (Figure 8) both exhibited saturation of magnetization at moderate field strengths indicating an absence of paramagnetic species (in contrast to the native sample). Field-cooled magnetization against applied field measurements (Figure 8b) indicated that there was no hysteresis loop shift indicating a lack of oxide layer around each cobalt particle.

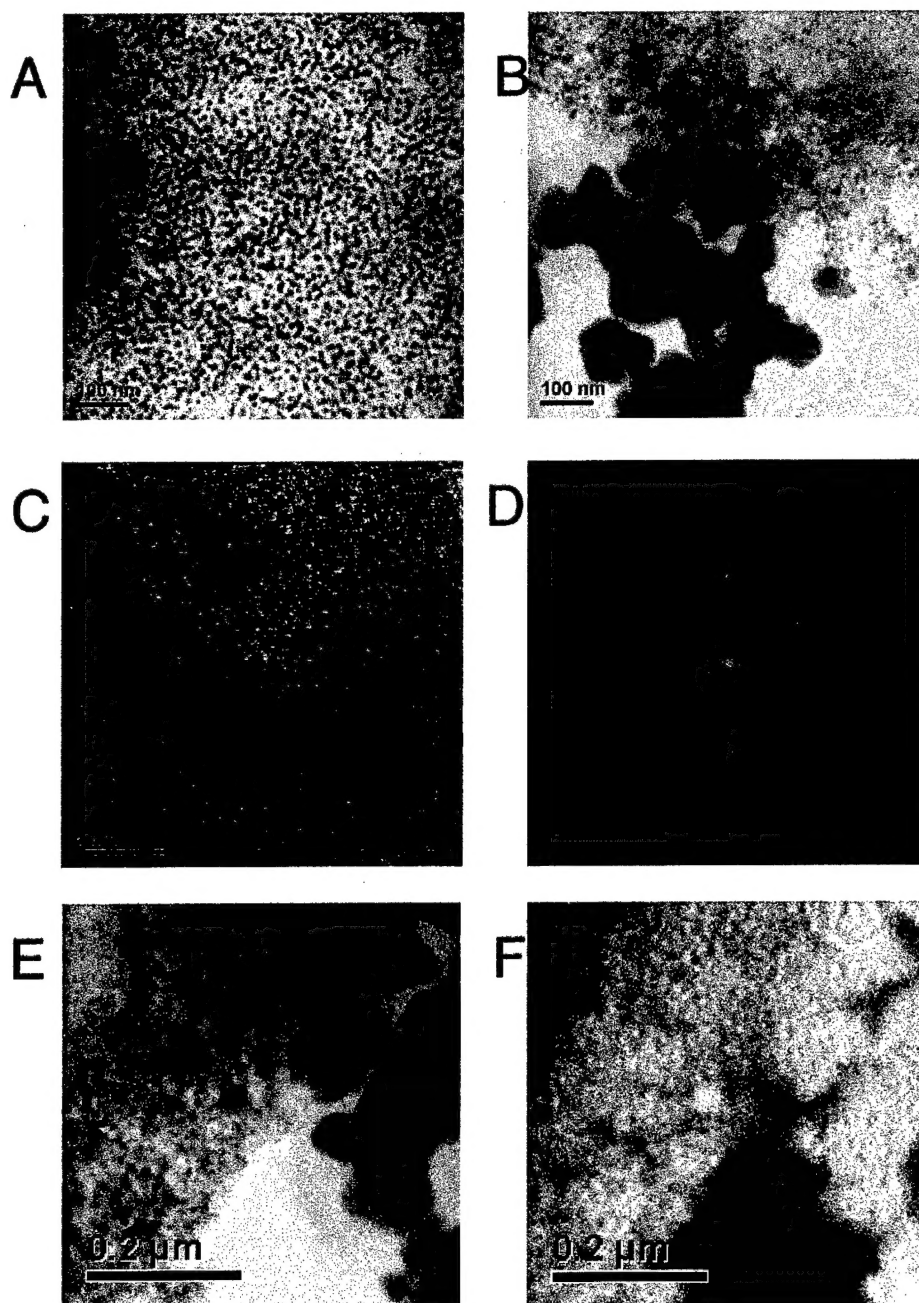


**Figure 6.** A JEOL 3000F field-emission transmission electron microscope was used to investigate the size and structure of cobalt nanoparticles prepared in toluene in the presence of PDMS-*b*-(PMVS-*co*-PMTMS) copolymer via thermolysis of  $\text{Co}_2(\text{CO})_8$ . A) bright field image of native sample, B) bright field image of pyrolyzed sample, C) high resolution image of pyrolyzed sample showing lattice planes of the crystalline cobalt particle, D) Fourier transform of (C), E, F) bright field image and cobalt elemental map of pyrolyzed sample using electron energy loss filter confirming particle identity.

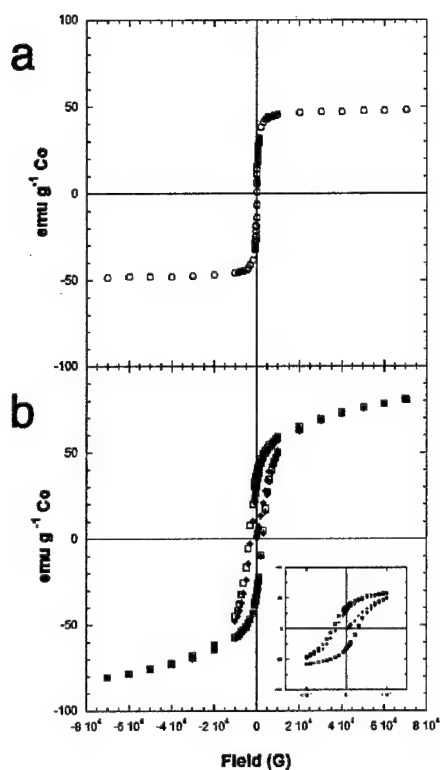


**Figure 7.**  $\sigma$  vs.  $H$  measurements conducted at a.) 300 K and b.) 5 K (zero field-cooled hysteresis loop  $\blacklozenge$ , field-cooled hysteresis loop  $\square$ ) on native sample of cobalt nanoparticles prepared in toluene in the presence of PDMS-*b*-(PMVS-*co*-PMTMS) copolymer via thermolysis of  $\text{Co}_2(\text{CO})_8$  and stored under argon. Inset in b) is enlarged region around the origin for 5 K hysteresis loops and shows no major asymmetric field-cooled hysteresis loop shift.

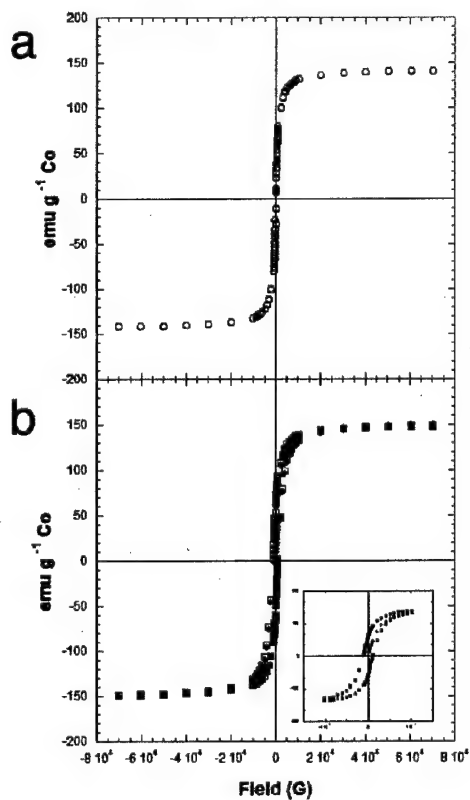


**Figure 8.**  $\sigma$  vs.  $H$  measurements conducted at a.) 300 K and b.) 5 K (zero field-cooled hysteresis loop  $\blacklozenge$ , field-cooled hysteresis loop  $\square$ ) on pyrolyzed sample of cobalt nanoparticles prepared in toluene in the presence of PDMS-*b*-(PMVS-*co*-PMTMS) copolymer via thermolysis of  $\text{Co}_2(\text{CO})_8$ . Inset in b) is enlarged region around the origin for 5 K hysteresis loops and shows no asymmetric field-cooled hysteresis loop shift.

Small angle x-ray scattering data from both the native and pyrolyzed samples were difficult to analyse quantitatively (Figure 9) but were consistent with the TEM observations. The data are consistent with a broadening of the particle size distribution on pyrolysis with the data from the pyrolysed sample possibly suggesting a bimodal distribution of particle sizes.

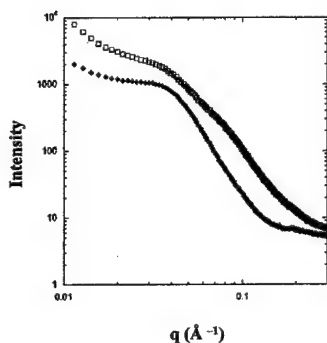


**Figure 9.** Small angle x-ray scattering measurements of native ( $\blacklozenge$ ) and pyrolyzed samples ( $\square$ ) of cobalt nanoparticles prepared in toluene in the presence of PDMS-*b*-(PMVS-co-PMTMS) copolymer via thermolysis of  $\text{Co}_2(\text{CO})_8$ .

In summary, the native cobalt nanoparticles prepared in toluene in the presence of PDMS-*b*-(PMVS-co-PMTMS) copolymer via thermolysis of  $\text{Co}_2(\text{CO})_8$  are weakly crystalline while their pyrolyzed counterparts appear more crystalline. Both TEM and SAXS indicate that the native particles have a narrow particle size distribution while the pyrolyzed particles appear to comprise a bimodal distribution of sizes. Pyrolysis of the native sample increases the cobalt specific saturation magnetization from approximately 48 emu/g Co to approximately 140 emu/g Co. An apparent paramagnetic component in the native sample, possibly unreacted cobalt carbonyl species, disappears upon pyrolysis.

### **Cobalt nanoparticles formed in poly(styrene-*b*-4-vinylphenoxyphthalonitrile) copolymer solutions: effect of pyrolysis on magnetic properties.**

Samples of cobalt nanoparticles formed in poly(styrene-*b*-4-vinylphenoxyphthalonitrile) copolymer solutions have been studied as synthesized (native) and after pyrolysis at 700°C. Details of the synthesis and pyrolysis procedures can be found in recent progress reports from Prof Judy Riffle and elsewhere (Baranauskas et al. 2004).

Measurements of the cobalt specific magnetization against applied field at room temperature indicate a large increase after pyrolysis (Figure 10). Further measurements have been made in order to elucidate the underlying cause of the increase in cobalt specific magnetization after pyrolysis.

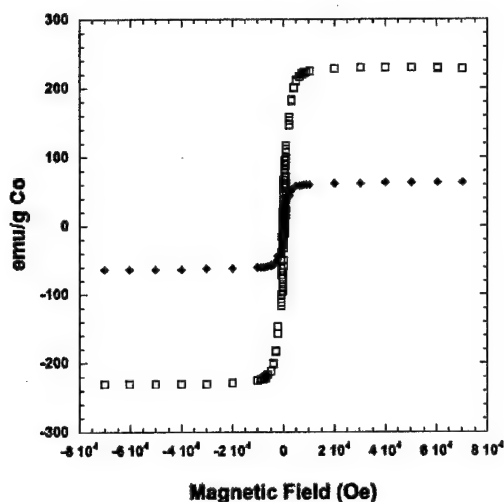


**Figure 10.** Cobalt specific magnetization vs applied magnetic field for native ( $\blacklozenge$ ) and pyrolysed ( $\square$ ) samples of cobalt nanoparticles formed in poly(styrene-*b*-4-vinylphenoxyphthalonitrile) copolymer solutions. Note that the absolute magnitude of the cobalt specific magnetization is dependent on a chemical analysis measurement (see later).

Transmission electron microscopy of the native sample supported on a carbon film indicates the formation of cobalt nanoparticles with dimensions on the order of 10 to 20 nm (Figure 11a). Figures 11b and 11c show a cobalt map and oxygen map of the same area of the TEM grid. The elemental maps were generated using electron energy loss filters. The cobalt image of Figure 11b appears to correspond closely to the electron density image of Figure 11a as expected. The oxygen image of Figure 11c appears to be more diffuse than either the electron density image or cobalt image suggesting that Figure 11c represents the spatial distribution of the polymer surrounding the cobalt particles. There will also be a contribution to the oxygen image from the oxidized surface layer on the cobalt particles (see later).

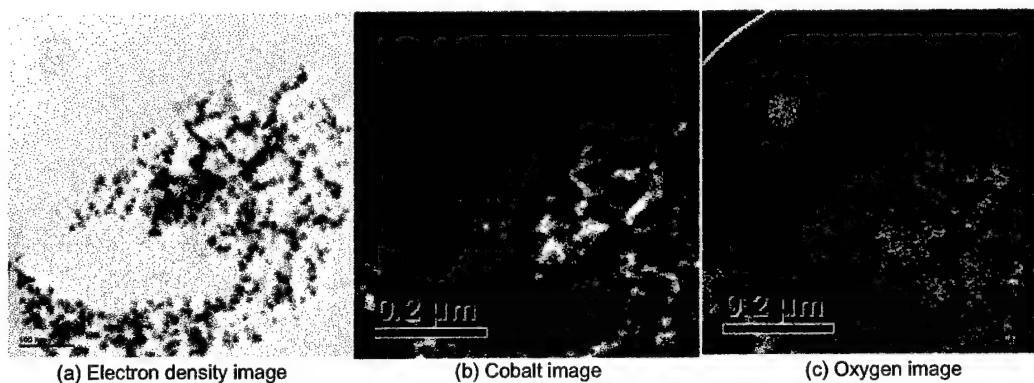


**Figure 11.** Transmission electron micrographs of native cobalt nanoparticles formed in poly(styrene-*b*-4-vinylphenoxyphthalonitrile) copolymer solutions.

Pyrolysis of the cobalt nanoparticles formed in poly(styrene-*b*-4-vinylphenoxyphthalonitrile) copolymer solution results in an aggregated mass which necessitates the use of thin sectioning techniques for TEM. TEM images from thin sections of the pyrolysed samples indicates particle sizes somewhat larger than those of the native sample (Figures 12 A, B, E, & F). High resolution TEM images reveal lattice planes within some particles (Figure 12 C). Fourier transforms of such images often reveal a single crystal character of the pyrolyzed particles (Figures 12 C & D).

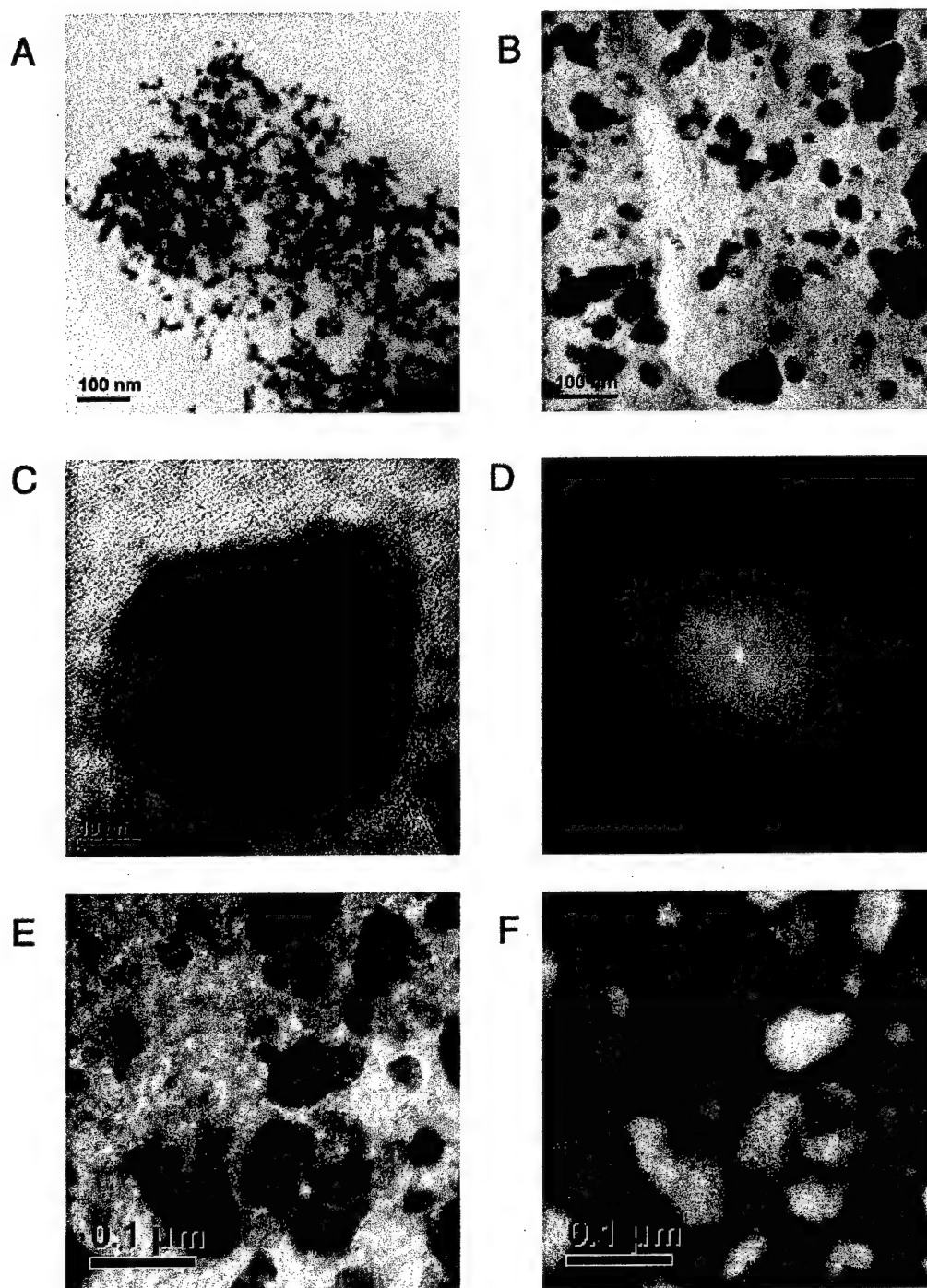


**Figure 12.** A JEOL 3000F field-emission transmission electron microscope was used to investigate the size and structure of cobalt nanoparticles formed in poly(styrene-*b*-4-vinylphenoxyphthalonitrile) copolymer solutions. A) bright field image of native sample, B) bright field image of pyrolyzed sample, C) high resolution image of pyrolyzed sample showing graphitic layers around the crystalline cobalt particle, D) Fourier transform of (C) showing crystallinity, E, F) bright field image and cobalt elemental map of pyrolyzed sample using electron energy loss filter confirming particle identity.

Magnetic susceptibility measurements were conducted on a dried pre-pyrolyzed sample that had been exposed to ambient conditions for three months. Room temperature measurements indicated a saturation magnetization of  $30 \text{ emu g}^{-1}$  material ( $80 \text{ emu g}^{-1} \text{ Co}$ ). A magnetic remanence of  $7 \text{ emu g}^{-1}$  material ( $19 \text{ emu g}^{-1} \text{ Co}$ ) and a coercivity of 410 Oe were observed indicating that a significant fraction of the sample was magnetically blocked at room temperature. Low temperature  $\sigma$  vs.  $H$  measurements indicated an asymmetric shift in the field-cooled hysteresis loop with respect to the zero field-cooled hysteresis loop (Figure 13). This loop shift is indicative of the coupling of an antiferromagnetic cobalt oxide layer with a ferromagnetic cobalt core (Nogues and Schuller 1999). This evidence supports the explanation for the decline in saturation magnetization over time being at least partially attributed to cobalt oxidation (Baranauskas et al. 2004). In addition, the cobalt specific magnetization ( $\sigma$ ) showed a continuous increase with field at high fields and low temperature. However, at room temperature  $\sigma$  almost saturated at high fields. These observations are consistent with the presence of paramagnetic species within the sample. This paramagnetic component is possibly due to residual cobalt species that have not been incorporated into the cobalt nano-crystals (Connolly et al. 2002; Connolly et al. 2004).

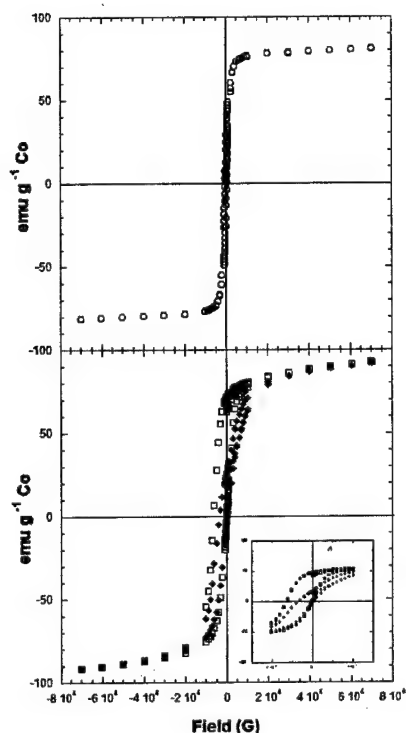


**Figure 13.**  $\sigma$  vs.  $H$  measurements conducted at a.) 300 K and b.) 5 K (zero-field cooled hysteresis loop  $\square$ , field-cooled hysteresis loop  $\blacklozenge$ ) on native sample of cobalt nanoparticles formed in poly(styrene-*b*-4-vinylphenoxyphthalonitrile) copolymer solutions. Inset in b) is enlarged region around the origin for 5 K hysteresis loops and shows an asymmetric field-cooled hysteresis loop shift. This is indicative of the coupling of a cobalt oxide layer (antiferromagnetic) with a cobalt core (ferromagnetic).

Magnetic susceptibility measurements were conducted on a pyrolyzed sample with block lengths of  $50,000 - 10,000 \text{ g mol}^{-1}$  poly(styrene-*b*-4-vinylphenoxyphthalonitrile) to further elucidate its magnetic properties (Figure 14). Two different values for cobalt specific saturation magnetization were obtained, associated with two different elemental analyses following two different sample digestion procedures denoted D1 for the 4-day digestion procedure and D2 for the 13-day digestion procedure. Sample preparation for the first analysis consisted of digesting a known amount of sample in 35 mL (volume over the total digestion period) of 1:1  $\text{HNO}_3\text{:H}_2\text{SO}_4$ . The sample was digested while heating at  $70\text{--}100^\circ\text{C}$  for 4 days. The sample for the second analysis was subjected to 35 mL of 1:1  $\text{HNO}_3\text{:H}_2\text{SO}_4$  for 13 days with an addition of 5 mL  $\text{H}_2\text{SO}_4$  added on the ninth day. The sample was heated at  $70\text{--}100^\circ\text{C}$  during the entire digestion process. The relatively robust nature of the protective graphitic coating is likely the explanation for the disagreement between the two sets of elemental analysis data. Graphite is an extremely stable and unreactive allotrope of carbon. Thus, it is reasonable that the graphitic type coating would passivate a metallic nanoparticle, protecting it from chemical reactions (e.g. oxidation). The more



rigorous digestion procedure for the second analysis resulted in higher calculated cobalt concentrations, suggesting that the protective coating can be digested over time under extreme conditions. Room temperature measurements showed apparent saturation magnetizations of  $230 \text{ emu g}^{-1}$  of calculated Co for D1 and  $172 \text{ emu g}^{-1}$  for D2. Both the magnitude of these values and their differences indicate that the sample digestion procedure for this material is critical to the values of cobalt concentration obtained from the ICP-AES measurements. The value of  $230 \text{ emu g}^{-1}$  Co for D1 is significantly higher than the maximum cobalt specific magnetization expected based on the value for bulk cobalt, and hence implies that the sample digestion was incomplete. The reduction in the apparent cobalt specific magnetization with increased digestion time suggests that the digestion process is very slow for this material.

Low temperature magnetization measurements on these pyrolyzed cobalt-graphitic complexes indicate similar saturation magnetizations. Field-cooled  $\sigma$  vs  $H$  measurements show magnetic hysteresis with negligible field bias relative to zero-field-cooled  $\sigma$  vs.  $H$  measurements (figure 11b), suggesting the absence of cobalt oxide layers around the metallic cobalt particles. The long-term saturation magnetization stability (Baranauskas et al. 2004) confirms that the pyrolyzed carbonaceous cobalt complexes are oxidatively stable. Compared to the pre-pyrolyzed sample, the cobalt specific magnetization for the pyrolyzed sample saturates at high fields in both room temperature and low temperature studies indicating an absence of the paramagnetic component that was observed for the pre-pyrolyzed sample. It is believed that residual carbonyl species evolve during the pyrolysis, and that this largely decreases or eliminates any paramagnetic species in the sample. Field-cooled and zero-field-cooled  $\sigma$  vs.  $T$  measurements in conjunction with  $\sigma$  vs.  $H$  measurements at room temperature suggest that both the pre-pyrolyzed and pyrolyzed samples consist of a combination of particles that are superparamagnetic and magnetically blocked at room temperature. Room temperature hysteresis loop measurements show that both samples exhibit magnetic remanence and coercivity (pre-pyrolyzed sample:  $H_c = 410 \text{ Oe}$ ,  $M_r = 19 \text{ emu g}^{-1} \text{ Co}$ ; pyrolyzed sample:  $H_c = 416 \text{ Oe}$ ,  $M_r = 34 \text{ emu g}^{-1} \text{ Co}$ ), values consistent with other cobalt nanoparticle preparations with similar size ranges e.g. (Sun and Murray 1999).

Transmission electron microscopy was employed to study the structure and morphology of the pyrolyzed cobalt-polymer composites. The particle size distribution was quite broad and suggested that some sintering had taken place during the heat treatment. The diffraction contrast across the large particles was continuous indicating that some small particles had indeed fused. The heat treatments resulted in complex crystalline particles, which have been difficult to classify uniquely as any of the known phases of cobalt (fcc, hcp or epsilon). Elemental mapping using a Gatan image filter (GIF) was used to confirm the elemental identity of the particles (Figure 12 F) before conducting high-resolution transmission electron microscopy (HRTEM). The sample consisted of highly crystalline particles, which facilitated the imaging of lattice fringes and "graphitic" coatings (Figure 12 C). The Fourier transform of the image in Figure 12 D indicates that the particles are strongly crystalline. The measured  $3.3 \text{ \AA}$  spacing for the inner ring of the Fourier transform is consistent with literature values for the interlayer spacing of graphite ( $3.4 \text{ \AA}$ ) (Terrones et al. 1997). The "graphitic" sheets follow the contour of the particle and may possibly act as the barrier that protects the particles against oxidation. Selected area electron diffraction (SAED) patterns were difficult to interpret owing to the complex nature of the crystalline cobalt particles so nano-beam electron diffraction (NBD), with a focused  $1.9\text{-nm}$  diameter probe, was used to obtain zone-axis diffraction patterns from individual crystal grains. The diffraction information from SAED and NBD, in conjunction with Fourier transforms of several crystalline particle images, suggest that the sample is comprised of a mixture of cobalt phases (fcc, hcp, epsilon and perhaps others). However, further study is required to ascertain the true crystallographic nature of the particles.



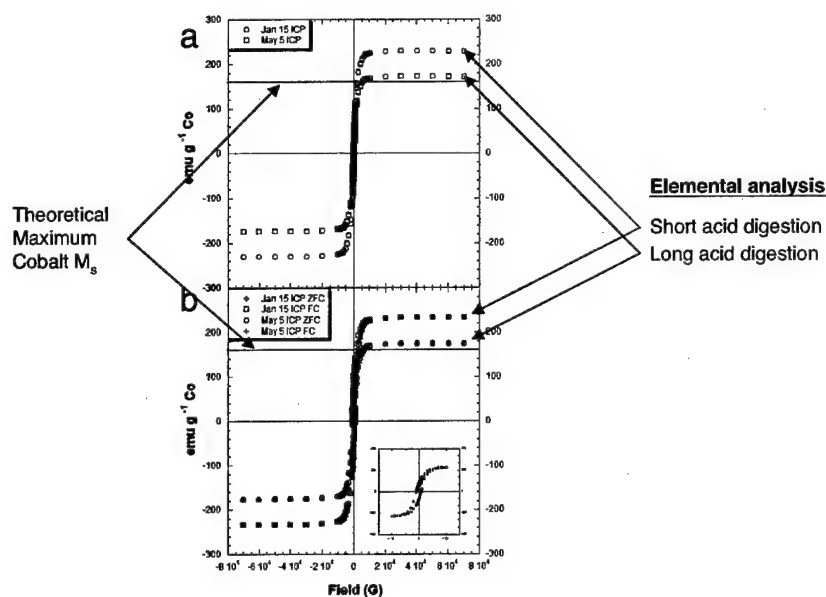


**Figure 14.**  $\sigma$  vs.  $H$  measurements conducted at a.) 300 K and b.) 5 K (ZFC – zero field-cooled; FC – field-cooled) on pyrolyzed sample of cobalt nanoparticles formed in poly(styrene-*b*-4-vinylphenoxyphthalonitrile) copolymer solutions. Inset in b) is enlarged region around the origin for 5 K hysteresis loops (Jan 15 ICP) and shows no asymmetric field-cooled hysteresis loop shift. Jan 15 ICP refers to one set of elemental analysis data while May 5 ICP refers to another. Note the discrepancy in  $M_s$  between the two sets of data.

Small angle x-ray scattering results of the native and pyrolyzed samples are shown in Figure 15. Analysis of the scattering data confirms that the native sample is in the form of nanoparticles with a relatively small range of particle sizes suggesting that the images obtained in Figures 11a and 12A are representative of the bulk of the sample. Small angle x-ray scattering from the pyrolyzed sample also indicates nanoscale structure (Figure 15). However, there is a clear difference in the SAXS data when compared with the native sample. The linear relationship between  $\log(I)$  and  $\log(q)$  over the range of  $q$  from 0.01 to approximately  $0.1 \text{ \AA}^{-1}$  suggests the formation of a fractal structure of electron density within the sample, possibly indicating the fusion of some of the particles.

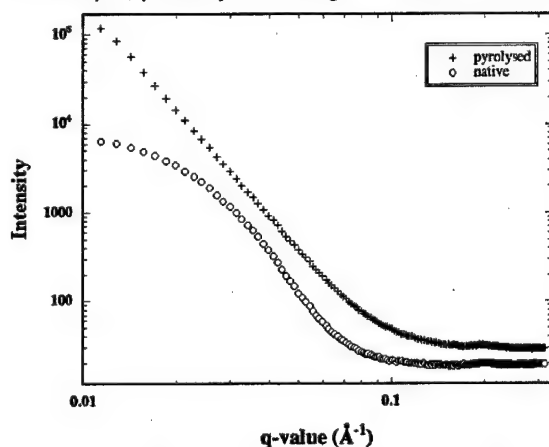


**Figure 15.** Small angle x-ray scattering from the native and pyrolyzed samples of cobalt nanoparticles formed in poly(styrene-*b*-4-vinylphenoxyphthalonitrile) copolymer solutions.

Magnetic measurements indicate that each sample contained both magnetically blocked and unblocked particles. Zero-field-cooled/field-cooled hysteresis loops measured for the native sample at 5 K exhibit large bias field shifts indicating the presence of exchange bias caused by the contact of antiferromagnetic and ferromagnetic substrates (Figure 16a). Such observations strongly suggest the layer of a cobalt oxide around each cobalt particle. However, similar measurements on the pyrolyzed sample (Figure 16b) showed no evidence for shifted field-cooled hysteresis loops, again suggesting that the graphitic coating protects the cobalt nanoparticles from oxidation.

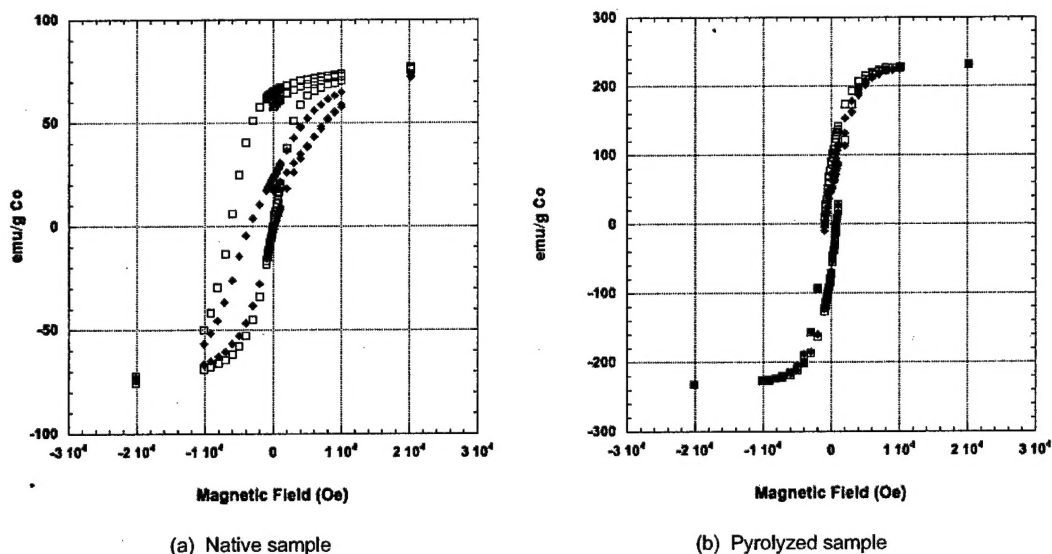


**Figure 16.** Zero-field-cooled ( $\blacklozenge$ ) and field-cooled ( $\square$ ) cobalt specific magnetization vs applied field at 5 K for samples of cobalt nanoparticles formed in poly(styrene-*b*-4-vinylphenoxyphthalonitrile) copolymer solutions

In summary, native cobalt nanoparticles formed in poly(styrene-*b*-4-vinylphenoxyphthalonitrile) copolymer solutions are weakly crystalline while their pyrolyzed counterparts have a high degree of crystallinity. The native particles have a narrow particle size distribution while pyrolysis appears to increase particle size and broaden the particle size distribution. Pyrolysis increases the cobalt specific saturation magnetization from approximately 80 emu/g Co to values close to that observed for bulk cobalt (160 emu/g Co). However, there is evidence that the carbon coating around the cobalt nanoparticles may cause erroneous elemental analysis results owing to the difficulty of digesting the graphitic coatings hence making measurements of cobalt specific magnetization problematical. A paramagnetic component of the native particles is absent in the pyrolyzed sample. The formation of a graphitic coating around the cobalt nanoparticles appears to prevent oxidation of the cobalt in air.

## References

- Baranauskas, V. V., M. A. Zalich, M. Saunders, T. G. St. Pierre and J. S. Riffle (2004). "Poly(styrene-b-4-vinylphenoxyphthalonitrile)-cobalt complexes and their conversion to oxidatively-stable cobalt nanoparticles." Chem Mater **submitted for publication**.
- Connolly, J., T. G. St Pierre, M. Rutnakornpituk and J. S. Riffle (2004). "Cobalt nanoparticles formed in polysiloxane copolymer micelles: Effect of production methods on magnetic properties." Journal of Physics D Applied Physics **37**: 2475-2482.
- Connolly, J., T. St. Pierre, M. Rutnakornpituk and J. S. Riffle (2002). "Silica coating of cobalt nanoparticles increases their magnetic and chemical stability for biomedical applications." European Cells and Materials **3**(Suppl. 2.): 106-109.
- Harris, L. A., J. D. Goff, A. Y. Carmichael, J. S. Riffle, J. J. Harburn, T. G. St Pierre and M. Saunders (2003). "Magnetite nanoparticle dispersions stabilized with triblock copolymers." Chemistry of Materials **15**(6): 1367-1377.
- Nogues, J. and I. K. Schuller (1999). "Exchange bias." Journal of Magnetism and Magnetic Materials **192**(2): 203-232.
- Sun, S. and C. B. Murray (1999). "Synthesis of monodisperse cobalt nanocrystals and their assembly into magnetic superlattices (invited)." Journal of Applied Physics **85**(8): 4325-4330.
- Terrones, M., N. Grobert, J. Olivares, J. P. Zhang, H. Terrones, K. Kordatos, W. K. Hsu, J. P. Hare, P. D. Townsend, K. Prassides, A. K. Cheetham, H. W. Kroto and D. R. M. Walton (1997). "Controlled production of aligned-nanotube bundles." Nature **388**: 52-55.
- Vadala, M. L., M. Rutnakornpituk, M. A. Zalich, T. G. St Pierre and J. S. Riffle (2004). "Block copolysiloxanes and their complexation with cobalt nanoparticles." Polymer **45**: 7449-7461.

## Personnel

The following professional personnel (based in Australia) were supported by and/or associated with the research effort:

Michael Zalich	Grad student
Dr Joan Connolly	Grad student
Dr Linda Harris	Post doctoral fellow
Dr Elliot Gilbert	Australian Nuclear Science and Technology Organisation
Dr Martin Saunders	Faculty
Nicole Gorham	Grad student/Research Associate
A/Prof Tim St Pierre	Faculty

Other personnel associated with the research effort were based at Virginia Tech in the laboratories of Prof Judy Riffle.

## Publications

The following papers have been submitted and/or accepted for peer-reviewed publication:

- Vadala, M.L., Zalich, M.A., Fulks, D.B., St. Pierre, T.G., Dailey, J.P., and Riffle, J.S. (2004) Cobalt-silica magnetic nanoparticles with functional surfaces. J. Mag. Magn. Mat., submitted.
- Harris, L.A., Riffle, J.S., and St. Pierre, T.G. (2004) Principles of design and synthesis of iron oxide magnetic nanoparticles for biomedical applications. J. Austral. Ceram. Soc., submitted.
- Baranauskas III, V.V., Zalich, M.A., Saunders, M., St. Pierre, T.G., and Riffle, J.S. (2004) Poly(styrene-*b*-4-vinylphenoxyphthalonitrile)-cobalt complexes and their conversion to oxidatively-stable cobalt nanoparticles. Chem. Mater., submitted.
- Vadala, M.L., Rutnakornpituk, M., Zalich, M.A., St. Pierre, T.G., and Riffle, J.S. (2004) Block copolysiloxanes and their complexation with cobalt nanoparticles. Polymer, 45, 7449-7461.
- Connolly, J., St. Pierre, T.G., Rutnakornpituk, M., Riffle, J.S. (2004) Cobalt nanoparticles formed in polysiloxane copolymer micelles: effect of production methods on magnetic properties. J. Phys. D: Appl. Phys., 37, 2475-2482.

## Interactions/Transitions

The following presentations were made during the year:

Physical Characterization of Nanoparticulate Cobalt/Polymer Complexes for Biomedical Applications  
M. A. Zalich, T. G. St. Pierre, V. V. Baranauskas, M. L. Vadala and J. S. Riffle. 5th International Conference on the Scientific and Clinical Applications of Magnetic Carriers, May 20 - 22, 2004, Lyon, France

Magnetic materials in medicine and biology. T.G. St Pierre. Japan Society for the Promotion of Science, 3<sup>rd</sup> Advanced Science Institute (Materials Science) Miyagi, Japan, July 25-31, 2004.

Nanoparticulate Cobalt/polymer Complexes for Biomedical Applications. M. Zalich, T. St. Pierre, J. Riffle and V. Baranauskas. Australian Institute of Physics 28th Annual Condensed Matter and Materials Meeting, Wagga Wagga, Australia, 3 - 6 February, 2004.

Physical Characterization of Nanoparticulate Cobalt/Polymer Complexes for Biomedical Applications. M. A. Zalich, M. Saunders, V. V. Baranauskas, M. L. Vadala, J. S. Riffle, T. G. St. Pierre. Australian X-ray Analytical Association - WASEM Joint Conference 2004, Rottnest Island, Western Australia, Sept 18th - 19<sup>th</sup>.

### **New discoveries, inventions, patent disclosures**

None